Biomaterials Science

Cell Resistant Zwitterionic Polyelectrolyte Coating Promotes Bacterial Attachment: An Adhesion Contradiction

Journal:	*Biomaterials Science*
Manuscript ID	BM-ART-12-2015-000585.R1
Article Type:	Paper
Date Submitted by the Author:	15-Jan-2016

Complete List of Authors:	Martinez, Jessica ; Florida State University, Biological Sciences Kelly, Kristopher; Florida State University, Chemistry and Biochemistry Ghoussoub, Yara; Florida State University, Department of Chemistry and Biochemistry Delgado, Jose; Florida State University, Chemistry and Biochemistry Keller, Thomas; Florida State University, Biological Sciences Schlenoff, Joseph; The Florida State University, Department of Chemistry and Biochemistry

Biomaterials Science

ARTICLE

Cell resistant zwitterionic polyelectrolyte coating promotes bacterial attachment: An adhesion contradiction

Received 00th January 20xx,
Accepted 00th January 20xx

DOI: 10.1039/x0xx00000x

www.rsc.org/

Jessica S. Martinez,[a] Kristopher D. Kelly,[b] Yara E. Ghoussoub,[b] Jose D. Delgado,[b] Thomas C. S. Keller III,[a] and Joseph B. Schlenoff[b]*

Polymers of various architectures with zwitterionic functionality have recently been shown to effectively suppress nonspecific fouling of surfaces by proteins and prokaryotic (bacteria) or eukaryotic (mammalian) cells as well as other microorganisms and environmental contaminants. In this work, zwitterionic copolymers were used to make thin coatings on substrates with the layer-by-layer method. Polyelectrolyte multilayers, PEMUs, were built with PAH [poly(allylamine hydrochloride)], PAH, and copolymers of acrylic acid and either the AEDAPS zwitterionic group 3-[2-(acrylamido)-ethyldimethyl ammonio] propane sulfonate (PAA-*co*-AEDAPS), or benzophenone (PAABp). Benzophenone allowed the PEMU to be toughened by photocrosslinking post-deposition. The attachment of two mammalian cell lines, rat aortic smooth muscle (A7r5) and mouse fibroblasts (3T3), and the biofilm-forming gram-negative bacteria *Escherichia coli* was studied on PEMUs terminated with PAA-*co*-AEDAPS. Consistent with earlier studies, it is shown that PAH/PAA-*co*-AEDAPS PEMUs resist the adhesion of mammalian cells, but, contrary to our initial hypothesis, are bacterial adhesive and significantly so after maximizing the surface presentation of PAA-*co*-AEDAPS. This unexpected contrast in the adhesive behavior of prokaryotic and eukaryotic cells is explained by differences in adhesion mechanisms as well as different responses to the topology and morphology of the multilayer surface.

Introduction

Biomaterial surface properties are key factors in clinical complications arising after implantation. Surfaces promoting adhesion and activation of macrophages and immune cells can trigger a foreign body acute inflammatory response that can persist for the lifetime of the medical implant, increasing mechanical wear and corrosion of the biomaterial thereby reducing its stability and overall lifespan.[1, 2] Adhesion of bacteria to prosthetics can cause additional complications. Development of bacterial biofilms (bacteria encased by a protective polymeric matrix) initiates when bacteria firmly attach to biotic or abiotic surfaces.[3] Many biofilms are resistant to antimicrobial agents (e.g. antibiotics) and the host immune response; treatment requires removal of the implant, subjecting a patient to additional surgeries and potential medical complications.[3, 4] Biofilms of *Escherichia coli*, *Staphylococcus epidermidis*, or *Staphylococcus aureus* are predominantly responsible for the numerous cases of bacterial infections of intravascular catheters and metal implants.[5-8]

Materials such as polymers and metals have been subjected to various types of surface modifications in recent years to improve surface chemistry and biocompatibility.[4, 9] FDA- and ISO-approved surface modifying methodologies include plasma spraying[10] or encasing biomaterials with hydroxyapatite coatings (e. g. plasma sprayed coating of hydroxyapatite).[11, 12] Emerging coating techniques use polyelectrolyte composites[13, 14] and layer-by-layer build-up[15-17] to coat medical devices with proteins or antibacterial components.

Polyelectrolyte multilayers (PEMUs) constructed layer-by-layer (LbL) with pairs of polyelectrolytes (PE) of alternating charge are biocompatible coatings stabilized by ion pairing interactions between the PE layers.[5, 18, 19] Assembly of PEMUs via the LbL process of dipping a surface into PE solutions is relatively inexpensive and ideal for coating irregularly shaped objects. PEMU surface properties can be tuned by varying the PE pairs and ionic/pH conditions in the LbL construction of the thin film coating.[20] Mechanical properties of PEMUs can be modified by introducing covalent bonds between the layers through thermal crosslinking,[21] chemical crosslinking,[22] or photocrosslinking,[23, 24] as in the PEMUs used in this investigation.

Zwitterionic functionality effectively prevents cell and protein adhesion to surfaces. Incorporation of various zwitterionic components into coatings has been shown to decrease adsorption of proteins,[25] attenuate immune

[a] Department of Biological Sciences, The Florida State University, Tallahassee, FL 32306, USA
[b] Department of Chemistry and Biochemistry, The Florida State University, Tallahassee, FL 32306, USA

Electronic Supplementary Information (ESI) available: FTIR detail of photocrosslinking; expanded time lapse images of aggregating bacteria; additional surface coverage data; cartoon of relative dimensions of cell and bacteria sitting on multilayers. See DOI: 10.1039/x0xx00000x

responses,[26-28] and resist attachment of eukaryotic cells[29, 30] and occasionally bacteria.[31] Zwitterionic repeat units, hydrophilic and net neutral,create a hydration layer thought to play an important role in resistance to protein absorption.[32] Zwitterion neutrality eliminates driving forces for protein adsorption due to counterion release.[25] Our previous investigations demonstrating that PEMUs containing the zwitterionic group 3-[2-(acrylamido)-ethyldimethyl ammonio] propane sulfonate (AEDAPS) are both protein and mammalian cell resistant,[29, 33] along with other reports on the nonfouling properties of zwitterions,[34, 35] led us to hypothesize that such a coating might also potentially resist prokaryotic (bacterial) cell attachment.

In this investigation, we compared attachment of rat aortic smooth muscle (A7r5) and mouse fibroblast (3T3) cells (representative of cell types associated with arterial stent failures[36, 37] and fibrous encapsulation[1, 2, 38] of implants, respectively) with attachment of biofilm-forming gram negative *Escherichia coli* enterobacteria to PEMUs of poly(allylamine hydrochloride) [PAH] and poly(acrylic acid) [PAA] containing the AEDAPS zwitterionic group at the outer surface. Because previous multilayers with increasing proportions of zwitterion had proven to be unstable,[29] a new approach of including photocrosslinkable stabilizing benzophenone groups was employed in the LbL construction of AEDAPS-containing PEMUs. Benzophenone was interspersed as comonomer units on one of the polyelectrolytes. Unexpectedly, AEDAPS PEMUS proved highly adherent for bacteria. In the present work, we describe simultaneous nonattachment by eukaryotic cells and strong affinity for prokaryotic cells and we discuss possible reasons for this difference.

Experimental

Reagents. Poly(allylamine hydrochloride) (molecular weight 56,000 g mol^{-1}), poly(acrylic acid) (molecular weight 100,000 g mol^{-1}, 47.2 wt% in water), sodium chloride (NaCl, 99.5%), sulfuric acid (H_2SO_4), *tris*(hydroxymethyl)aminomethane (Tris, $C_4H_{11}NO_3$ $\geq$ 99%), and hydrogen peroxide (H_2O_2) were used as received from Sigma Aldrich. PAA grafted with benzophenone (PAABp, benzophenone, Bp, is 18 mol% of the polymer, n = 0.82, m = 0.18), PAA grafted with AEDAPS (PAA-*co*-AEDAPS, AEDAPS is

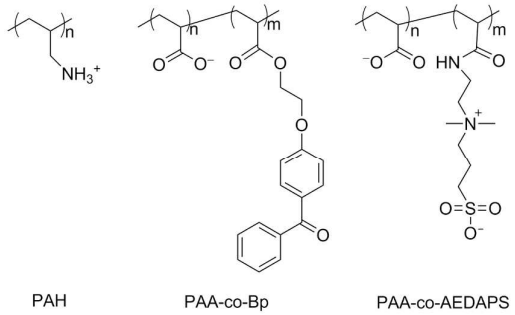

Scheme 1. Structures of polyelectrolytes employed.

25 mol% of polymer, n = 0.75, m = 0.25) were synthesized as described previously.[33, 39] All solutions were prepared using 18 MΩ deionized water (Barnstead, E-pure). Structures of polymers are shown in Scheme 1.

Double-side-polished silicon [100] wafers (100 mm) from Silicon, Inc., were divided into 22 x 22 mm squares, cleaned in "piranha" solution (70:30 H_2SO_4:H_2O_2, *caution*: strong acid and oxidizer) for 15 min, rinsed thoroughly with water, then dried under a stream of N_2. Microscope glass coverslips 22 x 22 x 0.17 mm (Fisherbrand Scientific cover slips No. 1) were flame cleaned for 1-2 seconds in three separate intervals.

LbL build-up of PEMUs was done as follows: Si wafers and glass coverslips were mounted onto glass microscope slides using Parafilm™ to hold the edges of the coverslips while exposing one side to solution during multilayer build-up. PEMUs were built using 10 mM (with respect to the repeat unit) PE solutions in 150 mM NaCl, 25 mM Tris, pH 7.3, with the aid of a robot (StratoSequence V, nanoStrata Inc.), which sequentially dipped the Si wafers and glass coverslips for 5 min into 50 mL of PE solutions and rinsed them for 1 min in 50 mL of 25 mM Tris, pH 7.3. After the final rinse, each PEMU was dried under N_2. No antimicrobial agents were used during the build-up of PEMUs. PEMUs were covered during and after build-up to prevent air particulate contamination. Personnel in direct contact with PEMUs used sterile laboratory practices, and contamination of solutions or PEMUs was extremely rare. All coated surfaces were stored dry in a sterile petri dishes sealed closed with Parafilm™ to prevent contamination (storage time ranged from a few days to a month at room temperature).

In the PEMU nomenclature used here, $(A/B)_m$-$(A/B\text{-}co\text{-}C)_n$ indicates a multilayer containing "m" bilayers of polycation *A* and polyanion *B*, and "n" bilayers of A and copolymer B-*co*-C. Photocrosslinked PEMUs are denoted as $(A/B)_m$-*X*-$(A/B\text{-}co\text{-}C)_n$. The PEMUs used for this investigation were: $(PAH/PAABp)_2$-X-$(PAH/PAA\text{-}co\text{-}AEDAPS)_4PAH$ (**AEDAPS-PAH**); $(PAH/PAABp)_2$-X-$(PAH/PAA\text{-}co\text{-}AEDAPS)_4PAABp$ (**AEDAPS-PAABp**); $(PAH/PAABp)_2$-X-$(PAH/PAA\text{-}co\text{-}AEDAPS)_4$ (**AEDAPS**); $(PAH/PAABp)_2$-X-$(PAH/PAA\text{-}co\text{-}AEDAPS)_4$ PEMU 'supplemental soaked' in PAA-*co*-AEDAPS for an additional 4 h (**AEDAPS-SS**). The PEMUs containing the base layers $(PAH/PAABp)_2$ were photocrosslinked in a UVP CL-1000 Ultraviolet Crosslinker as described previously[39] for 15 min at 200-280 nm before addition of the terminating layer. After buildup, with or without 'supplemental soaking', all PEMUs were rinsed with water and dried under a N_2 stream.

PEMUs were characterized by ellipsometry, static contact angle measurements, and Fourier transform infrared spectroscopy (FTIR). Dry thicknesses of PEMUs were determined using a Gaertner Scientific L116S Autogain ellipsometer with 632.8 nm radiation at 70° incident angle and a refractive index of 1.55. FTIR spectra of PEMUs were obtained at a resolution of 4 cm^{-1} with 100 scans using a Thermo Avatar 360 equipped with a DTGS detector. The background was determined using an uncoated (bare) Si wafer. All multilayer buildup and treatments were conducted at room temperature (23 ± 2 °C).

The dry surface roughness and thickness of PEMUs were determined using an MFP-3D atomic force microscope (AFM) (Asylum Research Inc., Santa Barbara, CA) equipped with an ARC2 controller. NCHV probes from Veeco (tip radius = 10 nm, spring constant 20–80 N m^{-1}) were used at a scan rate of 0.5 Hz. Images of 20 x 20 µm and 5 x 5 µm scan ranges were collected and then analyzed using Igor Pro software. Roughness was obtained from 5 x 5 µm regions (at different positions of 20 x 20 µm images). PEMUs thickness was determined by scanning the surface across a scratch made in the films and measuring the step height.

Mammalian cell culture. Rat aortic smooth muscle A7r5 cells and mouse fibroblast 3T3 cells (originally ATCC CRL-1444 and ATCC CRL-2752 respectively, both maintained through numerous passages and stored frozen in the lab over several years) were cultured on tissue culture plastic plates (TCP) in high glucose Dulbecco's Modified Eagle's Medium (DMEM) (D5648, Sigma-Aldrich) prepared from powder with sterile double distilled H_2O and supplemented with 1.5 g L^{-1} $NaHCO_3$, 10% fetal bovine serum (HyClone Standard Bovine Serum, Thermo Scientific), 10 µg mL^{-1} gentamicin (Gibco Gentamicin Reagent Solution, Invitrogen), and an antibiotic-antimycotic supplement providing final concentrations of 100 units mL^{-1} penicillin G, 100 µg mL^{-1} streptomycin, 0.25 µg mL^{-1} amphotericin (Gibco Antibiotic-Antimycotic, Invitrogen). The cells were cultured at 37 °C and 5% CO_2, refed every 3 days, and subcultured when populations were 70% confluent. For adhesion analysis, cells were trypsinized off TCP plates and plated onto uncoated and PEMU-coated glass coverslips.

***Escherichia coli* culture.** The ATCC-8739 *E. coli* strain of biofilm-forming gram negative enterobacteria (NCBI taxonomy ID 481805) used for this investigation was originally purchased from American Tissue Culture Collection, cultured in Luria Broth (LB) media in the lab, and stored as 40% glycerol stocks at -80 °C and on LB agar plates stored at 4 °C, which were replated on a monthly basis. *E. coli* used in fluorescent adhesion analyses were transformed with pGLO plasmid (Bio-Rad Laboratories). Concentrated culture suspensions were prepared from cultures inoculated with *E. coli* from a single colony into 1 mL of LB media in 1.5 mL microcentrifuge tubes kept at 37 °C with constant shaking (200 rpm) in a Thermo Scientific MaxQ 5000 Incubated/Refrigerated Floor Shaker for 12 h. *E. coli* concentrations in cultures were determined by measuring 600 nm light scattering using a ND-1000 NanoDrop Spectrophotometer (Thermo Scientific) assuming $1x10^8$ E.coli CFUs/mL/0.1 OD_{600} value.[40]

Live cell imaging and adhesion analysis. To facilitate DIC imaging of live mammalian cells and bacteria on uncoated and PEMU coated coverslips, sterile 35 mm tissue culture dishes were 'windowed' by drilling a hole with a variable speed bench drill press fitted with a 3/4" smooth-finish wood bit. The drilled culture dishes were sterilized with 70% ethanol, washed extensively with sterile PBS, and dried before gluing a PEMU coated or uncoated coverslip over the hole. The glue was allowed to cure for at least 24 h, after which the 'windowed' culture dishes were washed extensively with sterile PBS to remove any particulates. Alternatively, 35 mm glass bottom dish with a 20 mm micro-well sealed with a coverslip (#1 from In Vitro Scientific) were used.

Live cell imaging was conducted in a microscope-mounted LiveCell™ Chamber (Pathology Devices, Westminster, MD). During live cell recordings of mammalian cells, the chamber was maintained at 37 °C with 5% CO_2 input and 40% relative humidity. For live cell imaging of *E. coli* biofilm maturation, the chamber was maintained at 37 °C and 40% relative humidity, but no CO_2 was added into the chamber. Differences in reversible and irreversible attachment of *E. coli* under 'near static' conditions (some convection was caused by the influx of humidified air continuously pumped into the chamber) were recorded to analyze attachment of planktonic *E. coli* and subsequent biofilm formation during various periods after initial inoculation.

Mammalian cells and *E. coli* were imaged using a Nikon TS100 microscope equipped with a Nikon Digital Sight DS-Ri1 digital camera for Phase Contrast imaging and a Nikon Ti-E inverted microscope equipped with a Nikon Intensilight C-HGFI illuminator and a Photometrics Cool Snap HQ2 camera (Photometrics) for Differential Interference Contrast (DIC) and for Fluorescence imaging using Texas Red, DAPI, and GFP filters (Chroma Technologies Corp, EX: 560 nm, BS: 595nm, EM: 645 nm; EX: 350 nm, BS: 400nm, EM: 460 nm; EX: 470 nm, BS: 495nm, EM: 525 nm). Images were analyzed and processed using NIS-Elements Advanced Research (Nikon), ImageJ (NIH), and Adobe Photoshop.

***E. coli* attachment and retention analysis.** For adhesion assays, substrates were washed three times in 1 mL of phosphate buffered saline (PBS, pH 7.4) and soaked in 3 mL of PBS for 30 min at room temp before inoculating with 3 mL bacteria in LB media containing 5 x 10^4 E. coli CFU mL^{-1} or 7.7 x 10^6 *E. coli* CFU mL^{-1}. Cultures were maintained at 37 °C under static conditions for up to 48 h to allow formation of biofilms.

Surface coverage of tightly adherent *E. coli* after various times of incubation was analyzed by washing the surface with five rapid successive swirls in 1 mL PBS three times to remove non-adherent bacteria. Adherent bacteria were fixed and stained for 15 min with filtered 0.01% crystal violet prepared in PBS containing 20% methanol, destained with five rapid successive swirls in 1mL sterile deionized H_2O, and mounted with sterile gelvatol (13% v/v 1.5M Tris, pH 8.8; 21% v/v glycerol; 10.5% w/v polyvinyl alcohol; 0.02% w/v of sodium azide, NaN_3 prepared in deionized H_2O and stirred on low heat for 4 h). Prepared slides were imaged with the Nikon Ti-E and analyzed for relative coverage compared to uncoated coverslips with ImageJ (NIH).

Results and discussion

Following the discovery that the zwitterion functionality is highly effective at defeating non-specific adhesion/fouling of natural surfaces[41] many strategies for modifying synthetic polymers with zwitterions were reported.[42] One of the most effective approaches has been to grow brushes from surfaces using controlled polymerization methods. For example, Jiang's group[43] has reported inhibition of bacterial adhesion on

substrates grafted with poly(sulfobetaine methacrylate) brushes.[31] We introduced the use of zwitterion-modified copolyelectrolytes as an alternative for immobilizing sulfobetaine groups.[33] When combined with oppositely-charged polyelectrolytes in a thin multilayer these copolymers eliminated cell- and protein adhesion.[29] Some evidence was seen that the proportionate decrease of charged repeat units that comes with increasing zwitterion content leads to instability and loss of materials.[29] Thus, in the current work a new approach of including photocrosslinking benzophenone groups was employed.

The final multilayered film had the composition $(PAH/PAABp)_2$-$(PAH/PAA\text{-}co\text{-}AEDAPS)_4$. The first two bilayers were to provide a "base" of crosslinkable material on which to build four zwitterion-containing bilayers, terminated with zwitterion copolymer. The benzophenone content of the base layer, synthesized as previously described,[39] was rather high (18% measured by NMR) to promote extensive photocrosslinking. This crosslinking moiety was omitted from the top layers because it is known that polyelectrolytes in PEMUs interdiffuse about 3-4 bilayers.[44] For example, this level of interpenetration was demonstrated for multilayers of PAH and poly(styrene sulfonate).[45] Thus, a 4-bilayer PAH/PAA-*co*-AEDAPS cap should present no (hydrophobic) benzophenone at the surface.

Transmission FTIR of the final PEMU and comparison to reference spectra of the pure components revealed the composition of the PEMU (Figure S1). Exposing $(PAH/PAABp)_2$-$(PAH/PAA\text{-}co\text{-}AEDAPS)_4$ PEMUs to UV light (200-280 nm) produces a free radical on the Bp group of PAABp that drives random C-C crosslinking between layers within the PEMU.[39] A higher resolution FTIR spectrum comparing uncrosslinked to crosslinked $(PAH/PAABp)_2$-$(PAH/PAA\text{-}co\text{-}AEDAPS)_4$ PEMUs shows reduction of the Bp diarylketone peak after 15 min of UV exposure (see Supporting Information Figure S2) amounting to about 50% conversion of the Bp units.

A7r5 and 3T3 cell adhesion and spreading on zwitterionic surfaces

Previous findings by our group demonstrated that PEMUs terminated with zwitterionic PAA-*co*-AEDAPS (25 mol% AEDAPS) resist adhesion of both the extracellular matrix protein fibronectin and A7r5 rat aorta smooth muscle cells (SMCs).[29] The studies described here investigated adhesion of mammalian fibroblast 3T3 cells, representing a second type of clinically important cell line. In addition, time resolved analysis of cell adhesion demonstrates AEDAPS-directed resistance occurs during initial spreading and attachment and persists during longer incubation times. SMCs and 3T3 cells were individually seeded onto uncoated and AEDAPS-coated glass coverslips and imaged for 24 h (Figure 1). Cells from both lines began to attach and spread on the uncoated glass surfaces within 3 h of culture and continued to spread and increase attachment for the remaining time. In contrast, cells from both lines failed to adhere to the AEDAPS surface and instead aggregated into free-floating clusters.

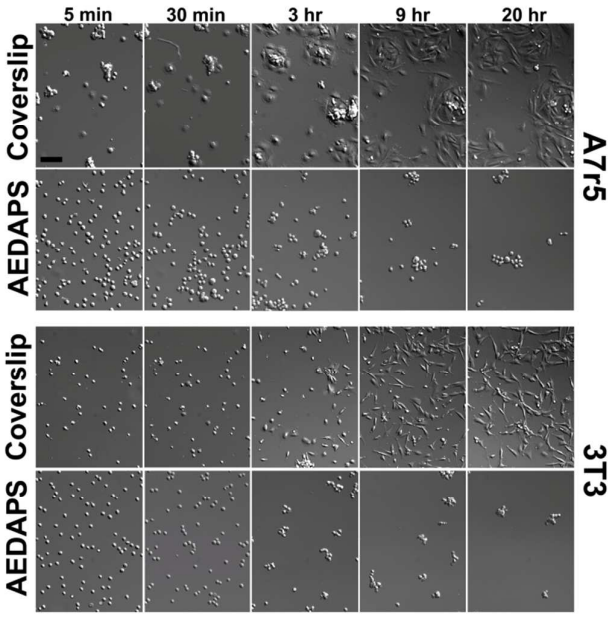

Fig. 1 Live A7r5 and 3T3 cells on uncoated and AEDAPS-coated coverslips. Cultured at 37° C with 40% relative humidity and 5% CO_2. Images are taken at 5 minutes and 3, 9, and 20 hours of culture. Scale bar is 100μm. See Supporting Information, Fig S3 for additional images taken at 30 minutes, 1, 6, and 15 hours and detail of A7r5 and 3T3 cells on control (bare coverslip) and AEDAPS-coated coverslips after 24 hours of culture.

The **AEDAPS** PEMUs used for this investigation were not directly cytotoxic.[18, 33] Other polymeric zwitterions also have negligible cytotoxicity.[46] When removed from the **AEDAPS** surface after 48 h in culture and replated onto tissue culture plastic the 3T3 cells in the clusters attached and migrated out of the cluster (Figure 2). Similarly, clustered A7r5 cells exposed to **AEDAPS** for 24 h adhered and spread when replated onto TCP. This is consistent with other studies demonstrating the effect of zwitterions, such as those on AEDAPS, on animal cell adhesion.[28-30, 33, 47] Unlike the 3T3 cells, however, extended **AEDAPS** exposure led to increased evidence of apoptosis in the clusters owing to the highly adhesion-dependent nature[36, 48, 49] of A7r5 cells (data not shown).

***E. coli* adhesion on zwitterionic surfaces**

Biofilm-forming bacterial substrate adhesion depends on a variety of factors, including the composition and amount of extracellular polymeric substances (EPS) surrounding the bacterium. EPS production can depend on growth conditions.[40, 50, 51] Before inoculation on the tested surfaces, the *E. coli* used here were grown to stationary phase, at which point the amount and composition of EPS they produce is conducive for substrate attachment and biofilm formation.[51] Irreversible attachment of *E. coli* onto a substrate is a critical variable in the development of biofilms that have extensive clinical consequences.[52-55]

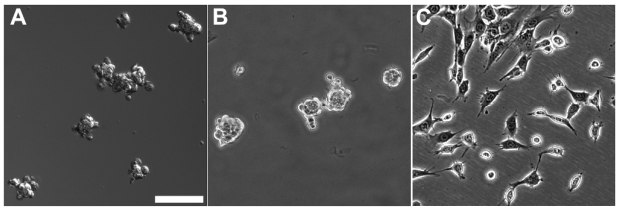

Fig. 2 Attachment and spreading on TCP of 3T3 cells cultured on AEDAPS coated coverslips. AEDAPS coated coverslips were seeded with 1 x 10^4 3T3 cells and cultured for 24 hours (A) and 48 hours (B) under normal tissue culture conditions. Cell clusters on AEDAPS surfaces after 48 hours were gently aspirated from the surface and replated and cultured for 24 hours on tissue culture plastic (C). Cells were imaged with DIC (A) and phase contrast (B and C) microscopy. Scale bar is 100µm.

To test whether the zwitterionic coatings also resist adhesion of biofilm-producing bacteria, sterile uncoated glass coverslips (as controls), and **AEDAPS** coated coverslips were inoculated with *E. coli* at a concentration of 5 x 10^4 CFU/mL. Under these 'static' conditions, the bacteria tended to grow as strands and clusters. Images of the cultures were recorded with DIC microscopy for 15 h (Figure 3). Bacteria in images taken every 15 min for 30 min time frames between 2 and 5.5 h of culture were pseudocolored blue for the first image, red for the image 15 min later, and green for the image 30 min after the first image of the group. The images were then merged to analyze immobilization of bacteria on these surfaces (Figure 3 and see Supporting Information Figure S3 and S4). Bacteria that were immobile despite subtle liquid convection in the growth chamber were clearly visualized as magenta (overlap of blue and red, indicating immobilization for only the first 15 min time period), yellow (overlap of red and green, indicating immobilization for only the second 15 min time period), and white (overlap of blue, red, and green, indicating immobilization for the entire 30 min time period). *E. coli* on **AEDAPS-SS** PEMUs began to establish robust irreversible attachments, which still allowed propagation, by 2 h in culture. Development of bacterial adhesion to the **AEDAPS** PEMU was delayed by close to 2 h, whereas bacteria were poorly immobilized on uncoated glass coverslip surfaces even after 5.5 h in culture.

The unexpected finding that bacteria bind avidly to **AEDAPS** prompted attempts to enhance the zwitterion content, thereby achieving the intended bacterial repellency, of the PEMUs by extended "supplemental soaking" in excess PAA-*co*-AEDAPS. The additional soaking of $(PAH/PAABp)_2$-$(PAH/PAA\text{-}co\text{-}AEDAPS)_4$ PEMUs in 10 mM PAA-*co*-AEDAPS for durations up to 16 h increases (then decreases slightly at the 16 h time point) the AEDAPS zwitterion concentration as demonstrated by increases in the AEDAPS FTIR absorption bands at 1050 and 1200 cm^{-1} (Figure 4). $(PAH/PAABp)_2$-$(PAH/PAA\text{-}co\text{-}AEDAPS)_4$ with 4 h supplemental soaking in PAA-*co*-AEDAPS are denoted as **AEDAPS-SS**.

Incorporation of additional PAA-*co*-AEDAPS in the AEDAPS-SS PEMUs was accompanied by significantly greater thickness and (less pronounced) changes in dry surface topography, without a significant change in the wettability as reflected by similar contact angles. The supplemental soaking caused a significant *increase* in bacterial attachment to the **AEDAPS-SS** PEMUs (Figure 3). Although at higher bacterial concentration

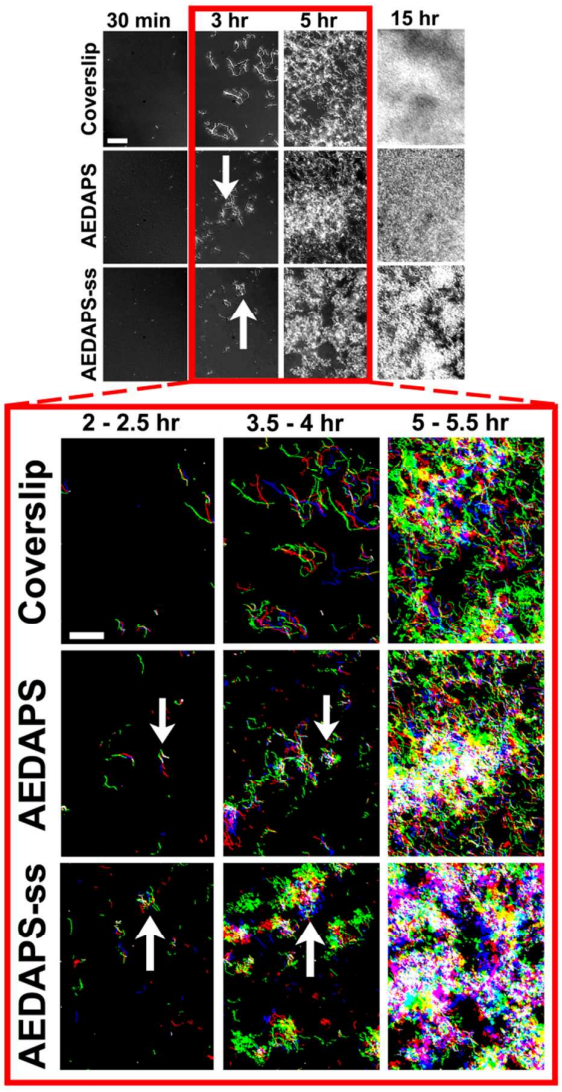

Fig. 3 *E. coli* adhesion over time on uncoated and **AEDAPS**, and **AEDAPS-SS** coated coverslips inoculated with 1.5 x 10^5 CFUs *E. coli* and imaged at 30 minute intervals. The 2-5.5 hour time frame from the upper panels is expanded in the lower panels, in which bacteria in three images for each of the time frames were pseudocolored blue (first image), red (15 minutes image), and green (30 minutes image) and merged to show bacteria pseudocolored magenta (blue and red overlap indicating immobilization only for the first 15 minutes time period), yellow (red and green overlap, indicating immobilization only for the second 15 minutes time period), and white (blue, red, and green overlap, indicating immobilization for the entire 30 minutes time period). White arrows in (A) and (B) point to regions on the **AEDAPS** and **AEDAPS-SS** surfaces where *E. coli* irreversibly attached and initiated biofilm formation. Scale bar is 50µm. For additional images and details of how merge images were created see Supporting Information, Fig S4, S5 and S6.

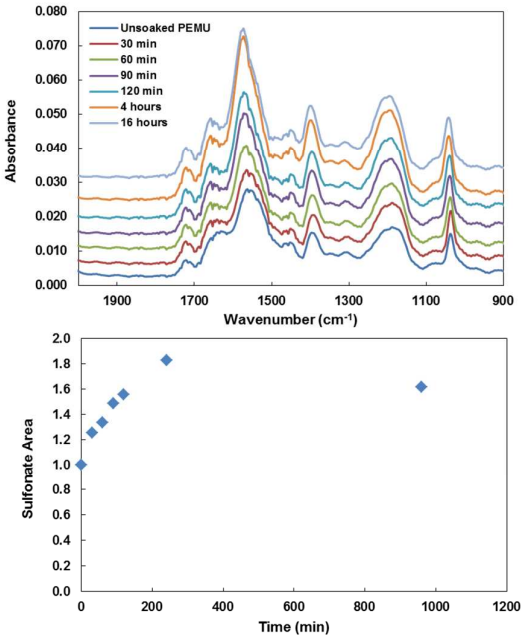

Fig. 4 Concentration of AEDAPS zwitterion increases in AEDAPS PEMUs with increased soaking time. AEDAPS PEMU was soaked in 10 mM PAA-*co*-AEDAPS polyelectrolyte solution (containing 150 mM NaCl and 25 mM Tris, pH 7.3). FTIR spectra after supplemental-soaking for: 0, 30, 60, and 90 minutes and 2, 4, and 16 hours, corresponding to the order of spectra from bottom to top (A) and areas of the sulfonate stretch at 1200 cm^{-1} for each time point (B).

there was little difference in the adhesion of the bacteria to **AEDAPS** and **AEDAPS-SS** PEMUs up to 30 min, at a lower concentration of bacteria, far more bacteria adhered sooner and more prolifically to **AEDAPS-SS** than to **AEDAPS**. The additional amount of **AEDAPS** absorbing into the **AEDAPS** PEMU, shown in Figure 4, reaches a limiting value then decreases slightly, suggesting the supplemental AEDAPS is loosely bound. The decrease in *E. coli* surface coverage percentages of **AEDAPS-SS** after 24 h might be a result of a bacteria-'trapping'-layer coming off with a loose **AEDAPS** layer, consistent with losses in polymer seen at longer times in Figure 4.

Considerable differences in bacteria exposure conditions exist in the literature on bacterial adhesion and biofilm formation. Often, surfaces are challenged with bacteria for only a few minutes then washed, which only provides information on the initial stages of planktonic attachment. In contrast, biofilms, which are more troublesome from a clinical standpoint, are typically formed over the course of a day or so. To compare short- and longer-term adhesion properties of zwitterion polymer films, **AEDAPS**, **AEDAPS-SS** and uncoated coverslips surfaces were inoculated with two bacterial concentrations then cultured for up to 30 min ("short" exposure) or 48 h ("long" exposure). The ATCC-8739 bacteria used for these investigations were transformed to express pGLO green fluorescent protein. Surfaces were inoculated with either 1.5 x 10^5 CFU *E. coli* ("low" concentration) or with 2.3 x 10^7 CFU *E. coli* ("high" concentration) under static culture conditions (no shaking). Prior to imaging the cultures were washed rigorously with swirling, which displaced more weakly adhered bacteria that were retained in the images in Figure 3. The bacterial surface coverage percentage was calculated for each surface (duplicates at each time point; Figure 5 and see Supporting Information Figure S5).

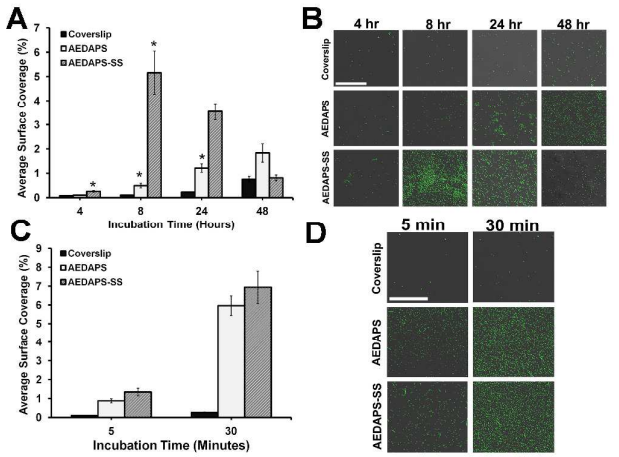

Fig. 5 Inoculation concentration dependence of tightly adhered bacteria surface on uncoated and **AEDAPS** and **AEDAPS-SS** coated coverslips. Average surface coverage percentages of *E. coli* expressing pGLO fluorescent protein, after 4, 8, 24, and 48 hours of static incubation with (A, B) compared to 5 and 30 minutes static incubations of *E. coli*, inoculated with 2.3 x 10^7 CFUs (C, D). DIC and fluorescent (GFP) images were merged for each condition tested (B, D). Surface coverage percentages were calculated using ImageJ (see Supporting Information, Fig S7). to measure the total surface area covered with *E. coli* on 0.15 mm^2 areas of images (n=10) for 2 trials. (*) indicates P values of <0.05 compared to average surface coverage percentage on uncoated coverslips and other tested surfaces. Scale bar 100µm.

The percentage of surface covered by tightly adhered bacteria increased with increasing incubation time for the control (glass) and **AEDAPS** surfaces. The ability of the zwitterion surfaces to *support* (instead of *suppress*) bacterial adhesion is clearly evident. The addition of more zwitterion copolymer by supplemental soaking enhanced the takeup of bacteria: at the lower inoculation concentration, the bacterial surface coverage percentage was two-fold greater on **AEDAPS-SS** compared to **AEDAPS** after 4 h and ten-fold greater after 8 h of incubation (Figure 5). Interestingly, the bacterial surface coverage percentage after 8 h continued to increase on the **AEDAPS** and uncoated coverslips but decreased on **AEDAPS-SS** with incubation time until it was equivalent to that on the uncoated coverslips and two-fold lower than on **AEDAPS** by 48 h. *E. coli* coverages on **AEDAPS** and **AEDAPS-SS** PEMUs after 24 h were greater than those found for PAH/PAABp PEMUs containing no zwitterions and PEMUs containing zwitterions terminated with a net negative (PAABp) or positive (PAH)

polyelectrolyte, while no measurable difference was observed in suspended *E. coli* (Figure 5 A and B, Supporting Information Figure S6 and S7). The conclusion is that biofilm formation on the zwitterion surfaces is not suppressed over the long term and is, rather, substantially promoted in some cases.

Bacteria inoculated at the much higher concentration and cultured for 5 and 30 min showed more dramatic differences between control and coated surfaces (Figure 5C, D). These short times are less than the period needed for the bacteria to multiply significantly and reflect the physical and mechanical interactions of bacteria in their planktonic (individual) state with surfaces. A dense coverage of bacteria with relatively uniform distribution is seen on the PEMU surfaces in Figure 5D.

Possible attachment mechanisms

The mechanisms of zwitterion antifouling, recently reviewed,[25] include a strongly hydrophilic surface that offers no enthalpic driving forces for interactions with hydrophobic moieties, and a surface charge that approaches zero, which defeats ion-pairing driving forces based on electrostatics and entropic losses of bound counterion. These two mechanisms are expected to be in play for preventing nonspecific bacterial adhesion as well.

The process of initial bacterial attachment to surfaces is complex and depends on variables such as substrate hydrophobicity, chemical composition, modulus, and (nano)morphology.[16, 56,57-59] Reversible attachment of planktonic bacteria (phase one) is followed by the start of biofilm formation (phase two).[60] Prior work included a starting assumption that surfaces resistant to protein adsorption may also resist bacterial adhesion.[61, 62] This assumption was shown to be only partially justified. For example, surfaces coated with a monolayer of polyethylene oxide were effective at eliminating protein adsorption but the same surfaces challenged with bacteria required a physical detachment stimulus.[63] The adhesion of bacteria was partially reduced with zwitterionic monolayers in the study of Ostuni et al.[61] but not in the work of Tegoulia et al.[64] Jiang's group has recently shown that the *type* of zwitterion, when incorporated into a brush, is critical in preventing bacterial adhesion based on polysaccharide intermediates.[65]

Here, water contact angles were measured in an effort to identify a difference, compared to glass control, in "hydrophilicity" between surfaces responsible for the affinity of bacteria for the zwitterionic films. Supplemental soaking increases **AEDAPS** PEMU thickness, but has no detectable effect on the static contact angle (Table 1).

Table 1. PEMU Thickness and Contact Angle

Substrate	Thickness (Å)	Θ_c
Coverslip*	-	~0°
AEDAPS	1056 ± 6	10 ± 2°
AEDAPS-SS	1173 ± 16	10 ± 2°
$(PAH/PAABp)_2$	207 ± 2	66 ± 3°

* Θ_c too low to measure

AEDAPS and **AEDAPS-SS** PEMU static contact angles are significantly lower than that of the more hydrophobic $(PAH/PAABp)_2$ PEMU. The similarity between glass, **AEDAPS** and **AEDAPS-SS** in contact angles and the difference in their bacterial affinity does not support an adhesion mechanism based solely on hydrophilicity. Two mechanical/topological mechanisms have been advanced recently to account for differences in bacterial adhesion. First, extending from findings and arguments made with eukaryotic cells,[66] substrate stiffness is thought to influence adhesion. Greater bacterial adhesion was observed with increasing stiffness of PEMUs[67, 68] and hydrogels.[69] Stiffness, however, is sensed actively by mammalian cells whereas bacteria have less developed and less sophisticated cytosketeletal machinery to translate stiffness cues into cellular response. Second, topological differences at a scale smaller than the size of a bacterium (i.e. smaller than the obvious contribution of defects that are large enough to trap bacteria) have been suggested to play an important role in adhesion.[59 70]

AFM topographical analysis shows **AEDAPS-SS** PEMUs to have similar roughness and thicknesses compared to **AEDAPS** (Figure 6), although the features on AEDAPS were more granular (Figure 6). These PEMUs were rougher than uncoated glass coverslips (rms roughness of 0.3 nm).

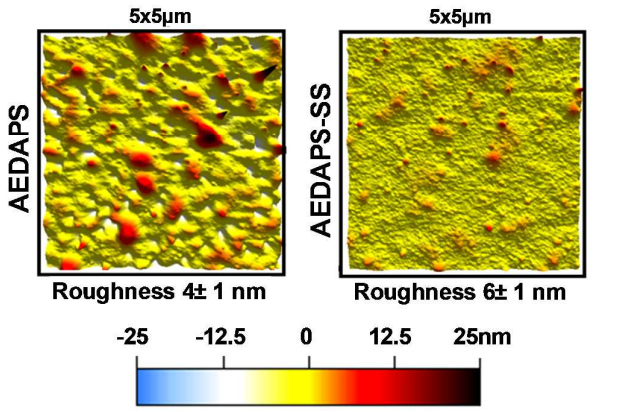

Fig. 6 AFM imaging of dry **AEDAPS** and **AEDAPS-SS** PEMUs. Dry thickness and surface roughness of photocrosslinked **AEDAPS** and **AEDAPS-SS** were measured using AFM (n=2 trials). **AEDAPS** PEMUs have an rms surface roughness of 4 ±1 nm, **AEDAPS-SS** PEMUs have a roughness of 6 ±1 nm.

The three dimensional topography of the zwitterion multilayers in Figure 6 is finer than the size of an *E. coli* bacterium. However, the nanometer scale surface peaks and valleys are comparable in size and spacing to *E. coli* fimbria (Supporting Information Figure S10 for illustration comparing *E. coli* and a mammalian cell interaction with the **AEDAPS-SS** PEMU surface). In addition, surfaces rich in zwitterions are likely to be softer because they are not ionically crosslinked like the bulk of the PEMU.[39] A combination of softness and nanoscale features may create an ideal environment where a

bacterium can engage the surface with its fimbria and maximize interactions. Because the additional copolymer introduced into the PEMU on supplemental soaking is loosely attached and the carboxylate repeat units not fully paired with polycation, the interactions are more extensive with **AEDAPS-SS**.

E. coli surface coverages on **AEDAPS** and **AEDAPS-SS** PEMUs after 24 h were greater compared to PAH/PAABp PEMUs containing no zwitterions and PEMUs containing zwitterions terminated with a net negative (PAABp) or positive (PAH) polyelectrolyte (Supporting Information Figure S5-S8). All surfaces were inoculated from a highly concentrated overnight culture ensuring a large dilution factor was used to neglect the influence of released glycoproteins and polysaccharides during initial attachment of *E. coli*. Increased *E. coli* attachment on AEDAPS surfaces was observed after 5 minutes of incubation (Fig 5) and irreversible attachment was observed after several hours of incubation (see Supporting Information Fig S4).

Surfaces showing vast differences between eukaryotic and bacterial attachment emphasize the differences in adhesion mechanisms between these two types of cells. Mammalian cells require firm adsorption of extracellular matrix (ECM) proteins such as fibronectin or collagen to a surface. During the initial stages of cell adhesion, transmembrane adhesion proteins, such as integrin, form specific binding interactions with these ECM proteins, activating integrins and subsequently upregulating nucleation of actin filaments at the periphery via activation of Cdc42 and Rac molecular signaling pathways.[71] These initial cell-ECM binding interactions help establish cell polarity as activation of Rho (signaling G-proteins) increases and stimulates formation of focal adhesion complexes.[72] Acto-myosin contractions generate intracellular tensile stress and cells begin to spread onto the surface.[73] Cells can also form nonspecific interactions with surfaces. Cell surface glycoproteins and oligosaccharides can form Van der Waals interactions with sugars, amino acids, and peptides such as arginine-glycine-aspartic acid (RGD) deposited on a surface.[74]

On the other hand, bacterial adhesion is more complex (or less understood), relying on a mix of interactions, including nonspecific electrostatic interactions which drive the development of irreversible attachment to surfaces during the early stages of bacterial adhesion.[54, 75, 76] Bacterial surface charge is provided by lipopolysaccharides (LPS) on the bacterial membrane.[77] Stationary bacteria (growth stage of *E. coli* used in this study) are more adhesive than mid-log-phase bacteria due to a higher degree of local charge heterogeneity.[51] Nonspecific physical interactions such as hydrophobicity,[78] roughness,[79] ionic strength,[80] and shear forces[81] affect bacterial attachment and biofilm formation. As bacteria form irreversibly attached microcolonies on surfaces, they become encased in polymeric matrix of sugars, DNA, and proteins (extracellular polymeric substance, EPS).[53] These microcolonies mature into macrocolonies, which release bacteria to re-enter the planktonic state, restarting the adhesion cycle.[52, 76, 82] Additionally, bacteria can exhibit specific interactions with other bacteria, substrate surfaces, or host cells through pili and fimbriae, which are surface adhesion appendages.[83] Fimbriae contain adhesins, protein structures that interact with certain molecules and amino acids driving attachment. For example, FimH adhesin on Fimbria type I selectively binds D-mannose, which has also been found to play a role in surface attachment.[83] Use of bacterial mutants and comparative studies with other gram-negative and gram-positive bacteria will better define the mechanism driving adhesion of *E. coli* on AEDAPS surfaces.

Thus far, the zwitterion coatings showing the greatest bacterial antifouling properties have been made of brushes, usually via "living" radical polymerization, extending from an attachment point at the surface.[31, 42] These high-performance brushes are of the same order of thickness as the PEMUs described here but they offer more dense coverage of zwitterions and they have no permanently charged co-units, such as the carboxylates in AEDAPS, that might exhibit electrostatic attractions with bacteria. In addition, the fact that brushes are usually dense and extended means fimbriae would find it more difficult to penetrate this excluded volume.

A surface treatment that resists the attachment of mammalian cells but encourages bacterial adhesion would not be considered suitable for coating implants. However, surfaces that promote bacterial attachment have potentially valuable niches in applications in fundamental studies, purification and filtration systems for mammalian cell "bioreactors," and even in biomedical engineering approaches, such as 'smart bandages', which draw out bacteria from a wound while preventing tissue growth around the bandage.[84, 85] AEDAPs PEMUs can help improve commercially available cell filters and strainers which purify cell samples for use in clinical and experimental applications. Additionally, bacterial films are useful in water and waste management[86], biofuel production[87], and even for designing enhanced coatings to test incorporation of bactericidal and bacteriostatic agents (i.e incorporation of metal nanoparticles[88]) or for the development of "living materials."[89]

Conclusions

It cannot be assumed that a surface which is highly effective at preventing protein and cell adhesion will also prevent biofouling by bacteria. For example, the zwitterion polymer coating described here is at opposite ends of the adhesion spectrum for the eukaryotic and prokaryotic cells studied. A survey of the literature on zwitterionic polymers suggests only the dense, neutral coating provided by a grafted polyzwitterion brush has so far provided complete antifouling properties against both cell types. These structure are absent in vivo because they would isolate cells from each other. For artificial surfaces the central challenge - generating dense zwitterion coverage - may be also be met by comb or dendrimer polymer architecture.

Acknowledgements

This work was supported in part by a grant from the National Science Foundation (DMR-0939850), and by the Florida State University.

Notes and references

1. J. M. Anderson, A. Rodriguez and D. T. Chang, *Seminars in Immunology*, 2008, **20**, 86-100.
2. J. M. Anderson, *Annual Review of Materials Research*, 2001, **31**, 81-110.
3. W. Zimmerli, A. Trampuz and P. E. Ochsner, *New England Journal of Medicine*, 2004, **351**, 1645-1654.
4. B. Jacobson and A. Murray, *Medical Devices: Use And Safety*, Churchill Livingstone, 2007.
5. F. Boulmedais, B. Frisch, O. Etienne, P. Lavalle, C. Picart, J. Ogier, J. C. Voegel, P. Schaaf and C. Egles, *Biomaterials*, 2004, **25**, 2003-2011.
6. L. A. Mermel, *Annals of Internal Medicine*, 2000, **132**, 391-402.
7. M. Ribeiro, F. J. Monteiro and M. P. Ferraz, *Biomatter*, 2012, **2**, 176-194.
8. V. Khanna, C. Mukhopadhayay, V. K. E, M. Verma and P. Dabke, *Journal of Pathogens*, 2013, **2013**, 936864.
9. A. Atala, R. Lanza, J. A. Thomson and R. Nerem, *Principles of Regenerative Medicine*, Academic Press, 2010.
10. Y. C. Tsui, C. Doyle and T. W. Clyne, *Biomaterials*, 1998, **19**, 2015-2029.
11. Y. Z. Yang, K. H. Kim and J. L. Ong, *Biomaterials*, 2005, **26**, 327-337.
12. P. K. Chu, J. Y. Chen, L. P. Wang and N. Huang, *Materials Science & Engineering R-Reports*, 2002, **36**, 143-206.
13. J. Jagur-Grodzinski, *Polymers for Advanced Technologies*, 2006, **17**, 395-418.
14. E. Khor and L. Y. Lim, *Biomaterials*, 2003, **24**, 2339-2349.
15. Z. Li, D. Lee, X. X. Sheng, R. E. Cohen and M. F. Rubner, *Langmuir*, 2006, **22**, 9820-9823.
16. J. A. Lichter, K. J. Van Vliet and M. F. Rubner, *Macromolecules*, 2009, **42**, 8573-8586.
17. K. Y. Cai, A. Rechtenbach, J. Y. Hao, J. Bossert and K. D. Jandt, *Biomaterials*, 2005, **26**, 5960-5971.
18. J. S. Martinez, T. C. S. Keller and J. B. Schlenoff, *Biomacromolecules*, 2011, **12**, 4063-4070.
19. J. D. Mendelsohn, S. Y. Yang, J. Hiller, A. I. Hochbaum and M. F. Rubner, *Biomacromolecules*, 2003, **4**, 96-106.
20. G. Decher and J. B. Schlenoff, *Multilayer Thin Films: Sequential Assembly of Nanocomposite Materials, 2nd Ed.*, Wiley-VCH, Weinheim, 2012.
21. J. J. Harris, P. M. DeRose and M. L. Bruening, *Journal of the American Chemical Society*, 1999, **121**, 1978-1979.
22. L. Richert, F. Boulmedais, P. Lavalle, J. Mutterer, E. Ferreux, G. Decher, P. Schaaf, J.-C. Voegel and C. Picart, *Biomacromolecules*, 2004, **5**, 284-294.
23. M. D. Moussallem, S. G. Olenych, S. L. Scott, T. C. S. Keller and J. B. Schlenoff, *Biomacromolecules*, 2009, **10**, 3062-3068.
24. A. Laschewsky, E. Wischerhoff, P. Bertrand and A. Delcorte, *Macromolecular Chemistry and Physics*, 1997, **198**, 3239-3253.
25. J. B. Schlenoff, *Langmuir*, 2014, **30**, 9625-9636.
26. J. Yuan, C. Mao, J. Zhou, J. Shen, S. C. Lin, W. Zhu and J. L. Fang, *Polymer International*, 2003, **52**, 1869-1875.
27. J. T. Sun, Z. Q. Yu, C. Y. Hong and C. Y. Pan, *Macromolecular Rapid Communications*, 2012, **33**, 811-818.
28. L. Zhang, Z. Cao, T. Bai, L. Carr, J.-R. Ella-Menye, C. Irvin, B. D. Ratner and S. Jiang, *Nature Biotechnology*, 2013, **31**, 553-+.
29. S. G. Olenych, M. D. Moussallem, D. S. Salloum, J. B. Schlenoff and T. C. S. Keller, *Biomacromolecules*, 2005, **6**, 3252-3258.
30. H.-W. Chien, C.-C. Tsai, W.-B. Tsai, M.-J. Wang, W.-H. Kuo, T.-C. Wei and S.-T. Huang, *Colloids and Surfaces B-Biointerfaces*, 2013, **107**, 152-159.
31. G. Cheng, Z. Zhang, S. F. Chen, J. D. Bryers and S. Y. Jiang, *Biomaterials*, 2007, **28**, 4192-4199.
32. S. F. Chen, L. Y. Li, C. Zhao and J. Zheng, *Polymer*, 2010, **51**, 5283-5293.
33. D. S. Salloum, S. G. Olenych, T. C. S. Keller and J. B. Schlenoff, *Biomacromolecules*, 2005, **6**, 161-167.
34. L. Xu, P. Ma, Q. Chen, S. Lin and J. Shen, *Progress in Chemistry*, 2014, **26**, 366-374.
35. M. Ilcikova, J. Tkac and P. Kasak, *Polymers*, 2015, **7**, 2344-2370.
36. S. O. Marx, H. Totary-Jain and A. R. Marks, *Circulation-Cardiovascular Interventions*, 2011, **4**, 104-111.
37. E. W. Raines, *International Journal of Experimental Pathology*, 2000, **81**, 173-182.
38. B. Rihova, *Advanced Drug Delivery Reviews*, 1996, **21**, 157-176.
39. A. M. Lehaf, M. D. Moussallem and J. B. Schlenoff, *Langmuir*, 2011, **27**, 4756-4763.
40. G. Sezonov, D. Joseleau-Petit and R. D'Ari, *Journal of Bacteriology*, 2007, **189**, 8746-8749.
41. R. F. A. Zwaal, P. Comfurius and L. L. M. Vandeenen, *Nature*, 1977, **268**, 358-360.
42. S. Jiang and Z. Cao, *Advanced Materials*, 2010, **22**, 920-932.
43. Z. Zhang, S. Chen, Y. Chang and S. Jiang, *The Journal of Physical Chemistry B*, 2006, **110**, 10799-10804.
44. G. Decher, *Science*, 1997, **277**, 1232-1237.
45. M. Lösche, J. Schmitt, G. Decher, W. G. Bouwman and K. Kjaer, *Macromolecules*, 1998, **31**, 8893-8906.
46. J. M. W. Chan, X. Ke, H. Sardon, A. C. Engler, Y. Y. Yang and J. L. Hedrick, *Chemical Science*, 2014, **5**, 3294-3300.
47. D. Du, J. Cai, H. X. Ju, F. Yan, J. Chen, X. Q. Jiang and H. Y. Chen, *Langmuir*, 2005, **21**, 8394-8399.
48. W. T. Gerthoffer, *Circ. Res.*, 2007, **100**, 607-621.
49. S. S. M. Rensen, P. Doevendans and G. van Eys, *Netherlands Heart Journal*, 2007, **15**, 100-108.
50. S. Tsuneda, H. Aikawa, H. Hayashi, A. Yuasa and A. Hirata, *Fems Microbiology Letters*, 2003, **223**, 287-292.
51. S. L. Walker, J. E. Hill, J. A. Redman and M. Elimelech, *Applied and Environmental Microbiology*, 2005, **71**, 3093-3099.
52. C. Beloin, A. Roux and J. M. Ghigo, *Bacterial Biofilms*, 2008, **322**, 249-289.
53. H. C. Flemming and J. Wingender, *Nature Reviews Microbiology*, 2010, **8**, 623-633.
54. O. E. Petrova and K. Sauer, *Journal of Bacteriology*, 2012, **194**, 2413-2425.
55. P. S. Stewart and J. W. Costerton, *Lancet*, 2001, **358**, 135-138.

56. Y. L. Ong, A. Razatos, G. Georgiou and M. M. Sharma, *Langmuir*, 1999, **15**, 2719-2725.
57. J. A. Lichter, M. T. Thompson, M. Delga-Dillo, T. Nishikawa, M. F. Rubner and K. J. Van Vliet, *Biomacromolecules*, 2008, **9**, 2967-2967.
58. T. J. Webster, C. Ergun, R. H. Doremus, R. W. Siegel and R. Bizios, *Journal of Biomedical Materials Research*, 2000, **51**, 475-483.
59. S. D. Puckett, E. Taylor, T. Raimondo and T. J. Webster, *Biomaterials*, 2010, **31**, 706-713.
60. Y. H. An and R. J. Friedman, *Journal of Biomedical Materials Research*, 1998, **43**, 338-348.
61. E. Ostuni, R. G. Chapman, M. N. Liang, G. Meluleni, G. Pier, D. E. Ingber and G. M. Whitesides, *Langmuir*, 2001, **17**, 6336-6343.
62. I. Banerjee, R. C. Pangule and R. S. Kane, *Advanced Materials*, 2011, **23**, 690-718.
63. A. Roosjen, H. C. van der Mei, H. J. Busscher and W. Norde, *Langmuir*, 2004, **20**, 10949-10955.
64. V. A. Tegoulia, W. Rao, A. T. Kalambur, J. F. Rabolt and S. L. Cooper, *Langmuir*, 2001, **17**, 4396-4404.
65. L. Mi, M. M. Giarmarco, Q. Shao and S. Jiang, *Biomaterials*, 2012, **33**, 2001-2006.
66. A. J. Engler, L. Richert, J. Y. Wong, C. Picart and D. E. Discher, *Surface Science*, 2004, **570**, 142-154.
67. J. A. Lichter, M. T. Thompson, M. Delgadillo, T. Nishikawa, M. F. Rubner and K. J. Van Vliet, *Biomacromolecules*, 2008, **9**, 1571-1578.
68. N. Saha, C. Monge, V. Dulong, C. Picart and K. Glinel, *Biomacromolecules*, 2013, **14**, 520-528.
69. K. W. Kolewe, S. R. Peyton and J. D. Schiffman, *ACS Applied Materials & Interfaces*, 2015, **7**, 19562-19569.
70. K. Bazaka, R. J. Crawford and E. P. Ivanova, *Biotechnology Journal*, 2011, **6**, 1103-1114.
71. L. S. Price, J. Leng, M. A. Schwartz and G. M. Bokoch, *Molecular Biology of the Cell*, 1998, **9**, 1863-1871.
72. K. Burridge and K. Wennerberg, *Cell*, 2004, **116**, 167-179.
73. M. ChrzanowskaWodnicka and K. Burridge, *Journal of Cell Biology*, 1996, **133**, 1403-1415.
74. W. F. Loomis, D. Fuller, E. Gutierrez, A. Groisman and W.-J. Rappel, *PLoS ONE*, 2012, **7**, e42033.
75. H. H. Tuson and D. B. Weibel, *Soft Matter*, 2013, **9**, 4368-4380.
76. J. Palmer, S. Flint and J. Brooks, *Journal of Industrial Microbiology & Biotechnology*, 2007, **34**, 577-588.
77. B. Vu, M. Chen, R. J. Crawford and E. P. Ivanova, *Molecules*, 2009, **14**, 2535-2554.
78. N. P. Boks, W. Norde, H. C. van der Mei and H. J. Busscher, *Microbiology-Sgm*, 2008, **154**, 3122-3133.
79. N. Mitik-Dineva, J. Wang, V. K. Truong, P. Stoddart, F. Malherbe, R. J. Crawford and E. P. Ivanova, *Current Microbiology*, 2009, **58**, 268-273.
80. X. X. Sheng, Y. P. Ting and S. O. Pehkonen, *J. Colloid Interface Sci.*, 2008, **321**, 256-264.
81. S. Lecuyer, R. Rusconi, Y. Shen, A. Forsyth, H. Vlamakis, R. Kolter and H. A. Stone, *Biophysical Journal*, 2011, **100**, 341-350.
82. A. Jain, Y. Gupta, R. Agrawal, P. Khare and S. K. Jain, *Critical Reviews in Therapeutic Drug Carrier Systems*, 2007, **24**, 393-443.
83. K. Otto, H. Elwing and M. Hermansson, *Colloids and Surfaces B-Biointerfaces*, 1999, **15**, 99-111.
84. M. Abrigo, P. Kingshott and S. L. McArthur, *ACS Applied Materials & Interfaces*, 2015, **7**, 7644-7652.
85. M. Abrigo, P. Kingshott and S. L. McArthur, *Biointerphases*, 2015, **10**, 04A301.
86. Z. Lewandowski, *Journal*, 2011, DOI: 10.1016/b978-0-444-53199-5.00095-6, 529-570.
87. Z.-W. Wang and S. Chen, *Applied Microbiology and Biotechnology*, 2009, **83**, 1-18.
88. S. Jaiswal, P. McHale and B. Duffy, *Colloids and Surfaces B: Biointerfaces*, 2012, **94**, 170-176.
89. A. Y. Chen, Z. Deng, A. N. Billings, U. O. S. Seker, Michelle Y. Lu, R. J. Citorik, B. Zakeri and T. K. Lu, *Nature Materials*, 2014, **13**, 515-523.

Cell Resistant Zwitterionic Polyelectrolyte Coating Promotes Bacterial Attachment: An Adhesion Contradiction

Jessica S. Martinez , Kristopher Kelly , Yara Ghoussoub , Jose D. Delgado , Thomas C. S. Keller III , and Joseph B. Schlenoff

Department of Biological Science and Department of Chemistry and Biochemistry,

Florida State University, Tallahassee, Florida 32306

TABLE OF CONTENTS GRAPHIC